Predicting Barrier Island Shrub Presence using Remote Sensing Products and Machine Learning Techniques

Benton Franklin[1], Laura J. Moore[1], and Julie C. Zinnert[2]

[1]Department of Earth, Marine, and Environmental Science, University of North Carolina at Chapel Hill, Chapel Hill, NC, USA

[2]Department of Biology, Virginia Commonwealth University, Richmond, VA, USA

Corresponding author: Benton Franklin (wbenton@email.unc.edu)

Key Points:

- Decision tree analysis and random forest modeling can predict shrub presence on barrier islands in Virginia with ~90% accuracy
- Shrub presence on barrier islands correlate with dune elevations >1.9 m and maintenance of island interior widths >160 m over a ~ 6-year period.
- Shrub establishment and removal lags changes in geomorphic conditions, indicating hysteresis

Abstract

Barrier islands are highly dynamic coastal landforms that are economically, ecologically, and societally important. Woody vegetation located within barrier island interiors can alter patterns of overwash, leading to periods of periodic barrier island retreat. Due to the interplay between island interior vegetation and patterns of barrier island migration, it is critical to better understand the factors controlling the presence of woody vegetation on barrier islands. To provide new insight into this topic, we use remote sensing data collected by LiDAR, LANDSAT, and aerial photography to measure shrub presence, coastal dune metrics, and island characteristics (e.g., beach width, island width) for an undeveloped mixed-energy barrier island system in Virginia along the US mid-Atlantic coast. We apply decision tree and random forest machine learning methods to identify new empirical relationships between island geomorphology and shrub presence. We find that shrubs are highly likely (90% likelihood) to be present in areas where dune elevations are above ~ 1.9 m and island interior widths are greater than ~160 m and that shrubs are unlikely (10% likelihood) to be present in areas where island interior widths are less than ~160 m regardless of dune elevation. Our machine learning predictions are 90% accurate for the Virginia Barrier Islands, with almost half of our incorrect predictions (5% of total transects) being attributable to system hysteresis; shrubs require time to adapt to changing conditions and therefore their growth and removal lags changes in island geomorphology, which can occur more rapidly.

Plain Language Summary

In this study we present two machine learning models for predicting the presence of shrubs on barrier islands. We use data derived from satellites, LiDAR, and arial imagery to create machine learning models. Using these models, we find that dune elevation and the minimum-island-interior width between surveys correlates with whether or not shrubs are present on barrier islands; sufficiently wide interior areas and sufficiently high dune elevations are necessary to support shrubs. Additionally, in certain areas we observe a lag between predicted and observed behavior. We attribute this lag to the different time scales over which shrub and barrier island geomorphology processes operate; barrier island geomorphology can change rapidly, but it can take several years for shrubs to respond to these changes.

Keywords:

Barrier island migration, machine learning, dune-shrub interactions, hysteresis

1 Introduction

Barrier islands are a common feature of coastal environments, located along roughly 10% of coastlines globally (Stutz & Pilkey, 2011). These highly dynamic landforms provide numerous societal benefits, including storm protection to mainland communities, tourism revenue, and nesting areas for ecologically important shorebirds. Aided by storms which cause overwash (e.g. Leatherman et al., 1979; Morton & Sallenger Jr, 2003), barrier islands migrate landward over time due to gradients in alongshore sediment transport (e.g. Cipriani & Stone, 2001; Fitzgerald et al., 1984; Robbins et al., 2022), decreases in sediment supply (e.g. Beets & van der Spek, 2000; Stutz & Pilkey, 2011; Williams et al., 2013), tidal inlet dynamics (e.g. Inman & Dolan, 1989; Leatherman et al., 1979; Nienhuis & Lorenzo-Trueba, 2019), and sea level rise (Lorenzo-Trueba & Ashton, 2014; Mariotti & Hein, 2022; Moore et al., 2010).

Coastal foredunes are prominent features on barrier islands and because water levels must exceed dune elevation for overwash to occur (Sallenger, 2000), dunes play a crucial role in determining how islands respond to storms (Durán Vinent & Moore, 2015) and how they migrate over time (Houser et al., 2018; Reeves et al., 2021). When dunes are overtopped and overwash occurs, sand is transported from the front of an island to its interior and beyond, resulting in landward barrier island migration in the case of sea-level rise and/or negative sediment supply (Donnelly et al., 2006; Leatherman, 1983). If islands are unable to move landward, they are at risk of drowning and disintegration (e.g. Lorenzo-Trueba & Ashton, 2014; Moore et al., 2010).

The presence of woody shrub vegetation on a barrier island can alter overwash dynamics by restricting sediment transport pathways in the island interior (Reeves et al., 2022; Zinnert et al., 2019). This disruption increases the likelihood of an island undergoing punctuated rather than continuous retreat, because shrubs inhibit overwash delivery to the island interior (Reeves et al., 2022). During punctuated retreat, barrier islands undergo alternating periods of landward migration followed by periods of relative immobility (Ashton & Lorenzo-Trueba, 2018; Ciarletta et al., 2019; Lorenzo-Trueba & Ashton, 2014).

Just as plant dynamics can alter barrier island response to storms (e.g. Durán Vinent & Moore, 2015; Reeves et al., 2022; Zinnert et al., 2019), storms can change barrier island plant communities. Storms can erode or wash away dunes (Morton & Sallenger Jr, 2003), removing established foredune vegetation and converting vegetated areas to bare sand (Snyder & Boss, 2002). Through the erosion and/or removal of foredunes, storms can also expose vegetation in the barrier island interior to salt spray, flooding, and burial (Carter et al., 2018; Snyder & Boss, 2002), potentially resulting in a decrease in total vegetated area and recolonization by more salt tolerant species. Over time, depending upon post-storm recovery rates, areas can return to prior ecological successions (Snyder & Boss, 2002; Velasquez-Montoya et al., 2021) or some habits may be eliminated (Carter et al., 2018).

Woody vegetation is a common ecological feature in coastal environments along the Gulf and East Coasts of the United States (Duncan & Duncan, 1987), establishing on barrier islands from seeds carried by wind, waves, and birds (Ehrenfeld, 1990; Shiflett & Young, 2010). On barrier islands, shrub growth has been linked to a variety of abiotic processes including warming climate (Huang et al., 2018; Wood et al., 2020), dune elevation (Woods et al., 2019), interior elevation (Young et al., 2011), salinity exposure (Young et al., 1994), and freshwater availability (Young et al., 2011). High dunes protect shrubs, especially seedlings, from salt spray and overwash (Miller et al., 2008); Woods et al. (2019) found foredune elevations of at least 1.75 m were required for shrub growth on the Virginia Barrier Islands, USA.

Several recent studies use a combination of LIDAR, aerial photography, satellite imagery, and field observations to classify landcover in a variety of barrier island settings (Anderson et al., 2016; Enwright et al., 2019; Fisher et al., 2023; Velasquez-Montoya et al., 2021). Although previous research succeeds in identifying the presence of vegetation and vegetation type, few studies predict its occurrence, though Enwright et al. (2019) succeeded in using machine learning techniques to predict 11 habitat classes on Dauphin Island, Alabama, including a woody vegetation class.

Because shrubs can alter the rate and style of barrier island migration (Reeves et al., 2022; Zinnert et al., 2019), our objective is to understand the relationship between barrier island geomorphology and the presence or absence of shrubs, and to develop a means for predicting shrub expansion and loss. Here we use decision tree analysis and random forest modeling—machine learning techniques—to assess the empirical relationships between barrier island geomorphology and shrub presence, and to identify remote-sensing-derived metrics capable of predicting the presence or absence of shrubs for large-scale undeveloped barrier island systems.

Machine learning techniques show promise in coastal geomorphology (e.g. Beuzen & Splinter, 2020; Houser et al., 2022). Recent examples include the use of machine learning to classify images to calculate coastal landslide risk (Fisher et al., 2023), characterize biological marsh communities (Martínez Prentice et al., 2021), and identify shoreline features (McAllister et al., 2022). Additionally, machine learning algorithms have been coupled with physically based models to predict changes in barrier island habitat (Enwright et al., 2021), calibrate dune evolution models (Itzkin et al., 2022), and simulate shoreline evolution (Montaño et al., 2020).

To meet our objectives, we focus on the Virginia Barrier Islands, which are largely owned by The Nature Conservancy (TNC) and are included within the National Science Foundation's Virginia Coast Reserve (VCR) Long-Term Ecological Research site. We focus on the islands that comprise the VCR, which extend 110 km along the outer coast of the DELMARVA Peninsula (Figure 1), from Fisherman's Island in the south to Metompkin Island in the north. Islands within the VCR are separated from the mainland by wide back-barrier lagoons many of which are fully or partially filled with back-barrier marsh (of varying width and depth).

Since 1962, the VCR has lost subaerial barrier island volume while simultaneously gaining shrub area (Zinnert et al., 2016). Because TNC owns the VCR and limits anthropogenic effects, the VCR is an ideal setting for studying natural physical and ecological barrier dynamics. While many other types of plants are found within the VCR, we focus on predicting the presence of shrubs because they are ubiquitous on many islands in the VCR (Zinnert, 2022; Zinnert et al., 2016, 2019) as well as other barrier islands in the U.S., and their presence significantly alters barrier island migration (Reeves et al., 2022; Zinnert et al., 2019).

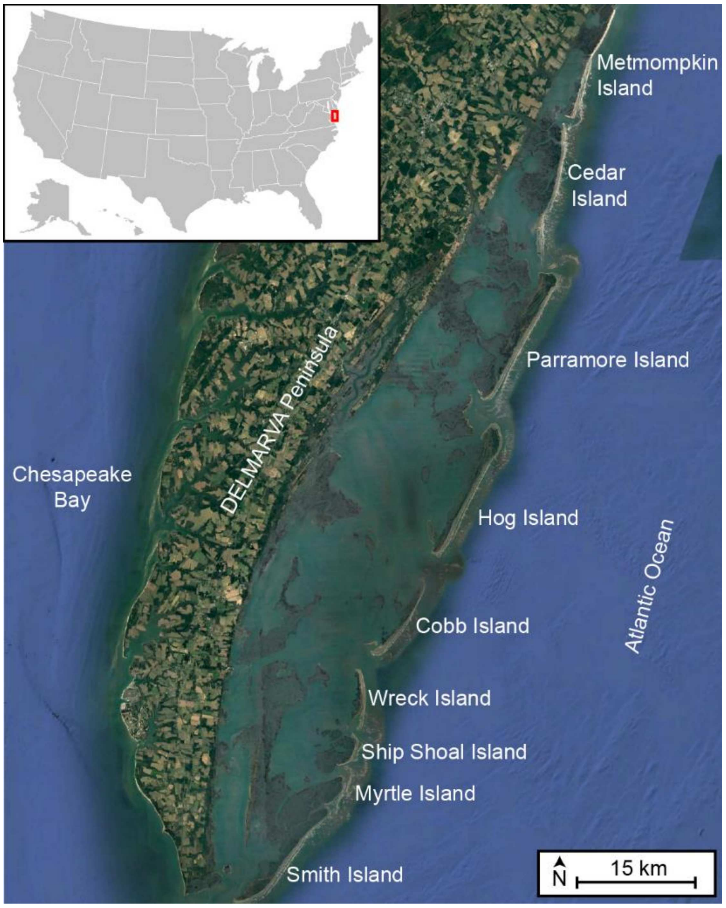

Figure 1. Study area map. The Virginia Coastal Reserve (VCR) extends from Smith Island to Metompkin Island, located on the Delmarva Peninsula, Virginia, United States.

2 Methods

2.1 Data

To quantify the relationship between barrier island geomorphology and shrub extent over space and time in the VCR, we utilized LiDAR digital elevation models (DEMs), landcover maps created from LANDSAT imagery by Zinnert et al. (2016, 2019, 2022), and aerial photography (Table 1). Three LiDAR DEMs from March 2010 (VITA, 2018), October 2016 (OCM Partners, 2023a), and June 2017 (OCM Partners, 2023b) allowed us to quantify dune morphometrics (details below). The 2010 DEM has a resolution of 3.048 m (10 ft) and a vertical accuracy of 20 cm, while the 2016 and 2017 DEMs have resolutions of 1 m and vertical accuracies of 10 cm. We supplemented DEM-derived values with dune elevations from Oster & Moore (2019), which were calculated from a 2005 United States Army Corps of Engineers (USACE) DEM with a 2 m resolution and a 20 cm vertical accuracy.

Table 1. Data sources. Summary of data type, collection year, accuracy, and source.

Remote Sensing Data	Year	Horizontal Accuracy	Data Sources
LiDAR	2005	2 m	Oster and Moore, 2007
	2010	3.048 m (10 ft)	VITA, 2011
	2016	1 m	OCM Partners, 2023a
	2017	1 m	OCM Partners, 2023ab
LANDSAT Groundcover	1998	30 m	Zinnert, 2022
	2011	30 m	Zinnert, 2022
	2016	30 m	Zinnert, 2022
Aerial Photography	2009	0.305 m	VGIN, 2009
	2013	0.305 m	VGIN, 2013
	2017	0.305 m	VGIN, 2017
	2021	0.305 m	VGIN, 2021

We identified the presence of shrubs using previously published landcover classifications generated by Zinnert et al. (2016, 2019, 2022) from LANDSAT (30-m resolution) using bands one through four, five and seven (resolution = 30m). Zinnert et al. (2016, 2019, 2022) divided the VCR into five landcover classes: woody, grassland, sand / bare, water, and marsh. All satellite images were collected between mid-August to mid-September, on cloud free days during the summer growing season (Zinnert et al., 2016) to minimize the effects of seasonal differences in vegetation cover. For this project, we focused on the woody, water, and marsh classes from 1998, 2011, and 2016, with shrubs being represented by the woody landcover class. We manually compared Zinnert et al.'s (2016, 2019, 2022) shrub classifications to true color and infrared aerial imagery from 2009, 2013, and 2017, with resolutions of 0.3 m collected by the Virginia Department of Emergency Management (Virginia Geographic Information Network, 2009, 2013, 2017), to serve as data validation. We used photographs collected in 2021 (Virginia Geographic Information Network, 2021) to gauge current shrub extent. All aerial photographs were collected in the spring, and although summer timing is more ideal, these are the only high-resolution aerial photographs available.

To efficiently analyze the large geographic area of the VCR, using ArcGIS Pro, we created 517 transects, spaced 100 m apart and spanning the eight VCR islands from Smith Island to Parramore Island. We cast transects perpendicular to a fixed offshore baseline that runs parallel to island shorelines, excluding transects that overlapped each other near inlets due to high inlet shoreline curvature, thereby avoiding the complexities associated with tidal inlet dynamics. To classify our transects as 'shrub' or 'non-shrub', we used the Zinnert et al. (2016, 2019, 2022) landcover classifications; we categorized transects as 'shrub' if they contained any amount of area classified as 'woody' landcover within 50 m of a transect, and conversely, we classified transects as 'non-shrub' if no shrubs were present. We chose a buffer of 50 m because our transects are spaced 100 m apart. Because shrub thickets are sometimes patchy, employing a 50-m buffer spacing allowed us to capture all areas with shrubs, while reducing the likelihood of counting the same area twice. Utilizing a buffer, rather than focusing on where transects directly intersect shrub polygons also allowed us to examine island and dune morphology characteristics for areas located near shrubs, and mitigated the lower 30-m spatial resolution of the shrub data (vs. aerial photography).

Because the LiDAR, LANDSAT, and aerial imagery were not all collected at a constant time interval, understanding temporal variability required us to create a composite time series representing conditions in 2010, 2016, and 2017 (Table 2).

Table 2. Summary of datasets (by year), used to generate annual composites. LiDAR (in bold italics) and LANDSAT (underlined) datasets identified by the year of collection, used to measure and develop the eight morphometric variables that characterize dune and island morphology. Note: When calculating the DCE_{LBS} for Composite 2017 we included 2010 as well as 2016 and 2017 because there was so little time between the 2016 and 2017 surveys, and therefore this doesn't capture the lowest value over a multi-year time span.

Datasets (*LiDAR*, LANDSAT)	Dune-crest elevation (DCE)	Lowest-dune-crest elevation between surveys (DCE_{LBS})	Island-interior width (IIW)	Minimum-island-interior width between surveys (IIW_{MBS})	Beach width (BW)	Change-in-dune-crest elevation (ΔDCE)	Change-in-island-interior width (ΔIIW)	Change-in-beach width (ΔBW)
2010 Composite	***2010***	***2005, 2010***	***2010***, 2011	(***2010***, 2011) vs (***2005***, 1998)	***2010***	***2010-2005***	(***2010***, 2011) - (***2005***, 1998)	***2010 - 2005***
2016 Composite	***2016***	***2010, 2016***	***2016***, 2016	(***2016***, 2016) vs (***2010***, 2011)	***2016***	***2016-2010***	(***2016***, 2016) - (***2010***, 2011)	***2016 - 2010***
2017 Composite	***2017***	***2010, 2016, 2017***	***2017***, 2016	(***2017***, 2016) vs (***2010***,2011)	***2017***	***2017-2010***	(***2017***, 2016) - (***2010***, 2011)	***2017 - 2010***

2.2 Morphometric Variables

To quantify dune and island interior characteristics (Table 2), we measured—for each composite data set—eight morphometric variables. We selected these variables because they can be reliably calculated and are potentially important to shrub presence (Figure 2). *Dune-crest elevation* (*DCE*) represents a transect's LiDAR-derived foredune elevation (Figure 2) which we identified using the Matlab program Automorph developed by Itzkin et al. (2020). Automorph identifies dune-crest elevation as the maximum seaward elevation found above a user-specified elevation (1.5 m for this analysis to avoid misidentifying berms as dunes) with a minimum backshore drop of 0.6 m behind it, based on formulations from Mull & Ruggiero (2014). *Lowest-dune-crest-elevation between surveys (DCE_{LBS})* represents the lowest dune-crest elevation value that we measured between the current and previous LANDSAT survey periods (e.g., for the 2016 composite, DCE_{LBS} is the lowest DCE measured from the 2010 and 2016 LiDAR surveys). *Island-interior width (IIW)* is the distance between the dune-crest elevation and the island interior edge (where the island interior intersects either the back-barrier bay or marsh edge if present), based on the boundary between marsh and water landcover classifications (Zinnert et al., 2016, 2019, 2022). We focus on the width of the island interior rather than total island width because shrubs only grow in the island interior. *Minimum-island-interior width between surveys (IIW_{MBS})* represents the smallest island-interior width measured for a transect between the current and previous LANDSAT surveys (e.g., for the 2016 composite, IIW_{MBS} is the smallest IIW between IIW 2010 and IIW 2016). *Beach width (BW)* is the distance between dune-crest elevation and the horizontal position where the elevation equals 0.35 m (NAVD88, representing mean high water used by Oster & Moore, 2019).

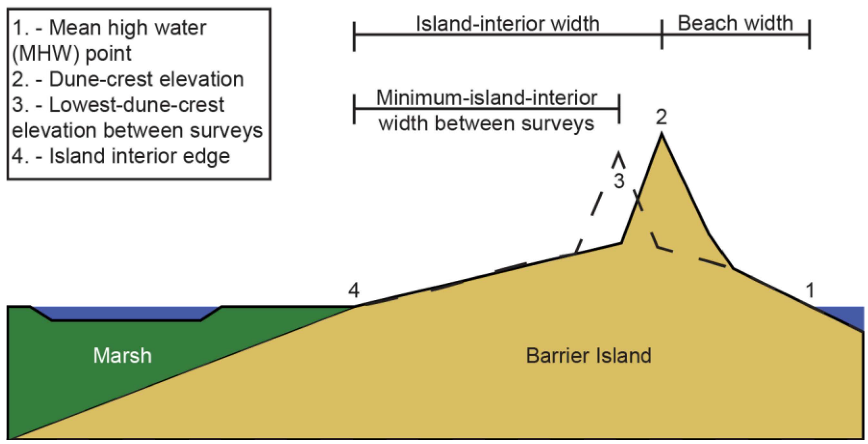

Figure 2. Illustration of morphometric variables. An idealized cartoon profile showing the location of each of the measured morphometric variables used to characterize dune and island morphology.

In addition to including measures of dune elevation, beach width, and island interior width, we quantified how these values changed over time. Because of differences in data set acquisition dates, we normalized our change-over-time variables to represent annualized percent change values. *Change-in-dune-crest elevation (ΔDCE)* represents the difference in DCEs between the current composite DCE value and previous composite survey DCE (e.g., ΔDCE 2016 is the difference between DCE 2016 and DCE 2010). We calculated *Change-in island-interior width* (*ΔIIW*) and *Change-in-beach width (ΔBW*) in the same way. Using the Mann-Whitney nonparametric test ($\alpha = 0.05$), we tested for statistically significant differences between shrub and non-shrub transects for each of the eight morphometric variables one at a time.

2.3 Machine Learning

Machine learning is a powerful tool that excels in identifying patterns within large datasets and that is commonly used to analyze data generated from remote sensed products (e.g., Barbarella et al., 2021; Gómez et al., 2022; Lary et al., 2016; Maxwell et al., 2018). These data-driven techniques have been used in a variety of coastal applications including the prediction of wave ripples (Goldstein et al., 2013), shoreline evolution (Montaño et al., 2020), and in the calibration of a physically based dune-beach model (Itzkin et al., 2022), among others. In this study, we use decision tree analysis and random forest modeling to categorize transects as either 'shrub' or 'non-shrub' based on our eight morphometric variables. While we initially considered utilizing several different machine learning techniques including support vector machine (SVM) and k-nearest neighbor (KNN) analysis, we elected to use decision tree analysis because it is easily interpreted and yields threshold values that can be further probed; we chose to use random forest modeling due to its high model accuracy and quick computation times.

We combined our three composite data sets (2010, 2016, 2017) in preparation for using machine learning and then, using R (version 4.1.1), we randomly split the data into training (75% of data) and validation sets (25% of data) (Figure 3). Although there are not specific rules on the sample size required to conduct machine learning analyses (Goldstein et al., 2019), improvements in model accuracy typically decrease and become marginal after reaching a certain threshold sample size (Luan et al., 2020; Morgan et al., 2003; Perry & Dickson, 2018). For example, Perry and Dickson (2018) used a small training set of approximately N=50 samples and found this sufficient for random forest model rankings of relative variable importance, with only minimal increases in model accuracy achieved by adding more samples. We sampled every 100 m within the VCR, because it afforded a sufficiently large dataset for performing training and validation, while simultaneously providing a small enough sample size to conduct quality control.

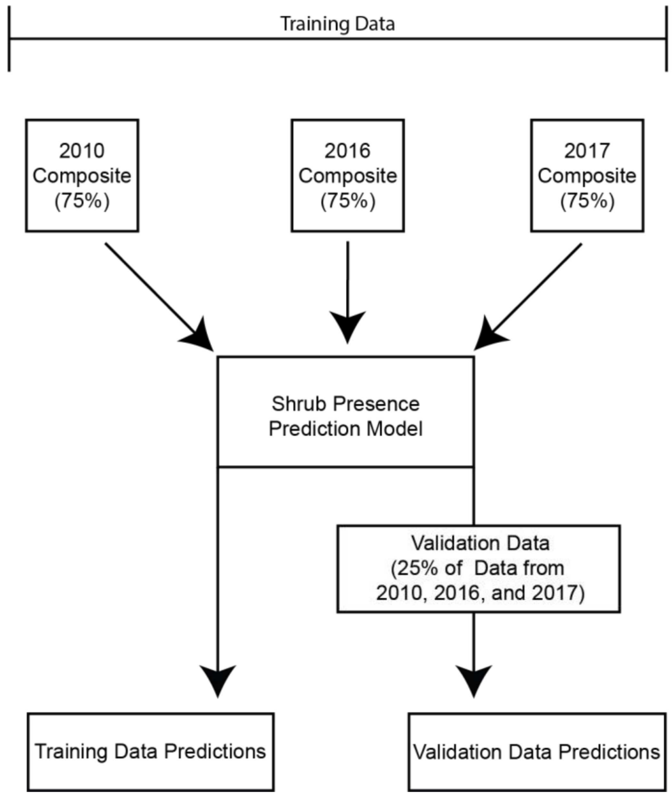

Figure 3. Machine learning workflow. 75% of the data comprising each composite was used to train the Shrub Presence Prediction Model which made the training data predictions. The remaining 25% of data not used to train our model was applied to generate validation data predictions.

2.3.1 Decision Tree Modeling

To conduct decision tree analysis we used the 'rpart' (Therneau et al., 2022) R package. Decision tree analysis repeatedly splits data into groups based on different explanatory variable values to find the combination of values that is best able to predict the presence of a response variable (Breiman et al., 1984; De'ath & Fabricius, 2000; Goldstein et al., 2019), while minimizing the number of output categories.

After completing decision tree modeling, we examined the misidentified transects to identify where predictions diverged from observations. In this analysis, we focused on three potential sources of error: system hysteresis, remote sensing misidentification, and decision tree misclassification. We considered a transect to be misclassified due to system hysteresis when observed shrub presence or absence on a transect did not match decision tree predictions but did match observations from LANDSAT or aerial imagery collected within the following 10 years. Remote sensing misidentification occurred when the LANDSAT-derived shrub classification for a given transect disagreed with higher resolution aerial imagery collected during the same period. To identify these instances, we compared 2016 LANDSAT imagery to 2017 aerial imagery, and the 2011 LANDSAT imagery to both 2009 and 2013 aerial imagery. We made this comparison, by overlaying Zinnert et al.'s (2022) shrub polygons on the corresponding aerial photographs in ArcGis Pro and visually inspecting the transect locations to determine if shrubs were, in fact, present in the locations indicated by the LANDSAT imagery analysis. We refer to prediction errors that we couldn't attribute to either hysteresis or remote sensing misclassification, as decision tree errors.

2.3.2 Random Forest Modeling

For comparison with the results of the decision tree analysis and to gauge the relative importance of the eight morphometric variables, we conducted random forest (RF) modeling using the 'randomForest' (Liaw & Wiener, 2022) R package. RF modeling is an expanded form of decision tree analysis (Breiman, 2001; Hastie et al., 2009). RF models create a series, or 'forest,' of different decision trees, each drawn from a randomly sampled subset of the training data response variables. Each individual decision tree within the 'forest' results in a prediction based on its response variables, with the random forest model averaging together the predictions from each individual tree to make an overall classification based on the predictions of a majority of trees. Informed by the work of Oshiro et al. (2012) who found 64-128 trees sufficient to make accurate predictions, we chose to use the R package default of 500 trees. This far surpasses the minimum number of trees recommended by Oshiro et al. (2012), yet still allows reasonably rapid computation time.

2.4 Analyzing Shrub Colonization and Removal for Comparison with DT Thresholds

To gauge the accuracy of DT-generated empirical thresholds for predicting shrub colonization or removal, we analyzed transects that changed shrub classification, examining dune-crest elevation and minimum-island-interior width between survey values. We identified 'shrub colonization' and 'shrub loss' transects using ArcGIS Pro, overlaying shrub polygons from Zinnert et al. (2022) from 1998, 2011, and 2016 to identify areas of shrub loss or expansion. We compared the 1998 and 2010 LANDSAT surveys to determine change for the 2010 composite transects and used the 2011 and 2016 surveys for the 2016 and 2017 composite transects. Based on this analysis, we considered transects that lacked (had) shrubs in the previous LANDSAT survey but have (lack) shrubs in the subsequent LANDSAT survey to represent 'shrub colonization' ('shrub removal') transects. To ensure accuracy, we then verified the presence or absence of shrubs for each transect by visually comparing Zinnert et al.'s (2022) woody classification polygons to aerial photographs taken around the same time, using the same image comparison procedure outlined earlier, retaining verified transects for further analysis as mentioned above.

3 Results

3.1 Morphometric Variables Statistical Analysis

Shrub and non-shrub transects were statistically different from each other across most of the measured dune and island-interior morphometrics. Comparing dune morphometrics between shrub and non-shrub transects using the Mann-Whitney (MW) test revealed that shrub transects had higher dune-crest elevations (shrub mean = 2.58 m +/- 0.53, non-shrub mean = 1.85 m +/- 0.39, $p_{MW} < 0.01$; Figure 4a) than non-shrub transects, as well as higher lowest-dune-crest elevation between surveys values (shrub mean = 2.13 m +/- 0.46, non-shrub mean = 1.59 m +/- 0.36, $p_{MW} < 0.01$; Figure 4b), and greater changes in dune-crest elevation (shrub mean = 0.04% +/- 0.76%, non-shrub mean = -0.01% +/- 0.54%, $p_{MW} < 0.01$; Figure 4c). Comparison of island-interior morphometrics for shrub vs. non-shrub transects revealed a similar pattern; relative to non-shrub transects, shrub transects had greater island interior widths (shrub mean = 501m +/- 318, non-shrub mean = 132 m +/- 155, $p_{MW} < 0.01$; Figure 4d) and higher minimum-island-interior-width-between survey values (shrub mean = 489 m +/- 322, non-shrub mean = 93 m +/- 141, $p_{MW} < 0.01$; Figure 4e). In contrast, non-shrub transects, in comparison to shrub transects, had greater beach widths (shrub mean = 7.2 +/- 17.3, non-shrub mean = 27.4 m +/- 47.0, $p_{MW} <$ 0.01; Figure 4f) and change-in-island-interior widths (shrub mean = 2% +/- 549%, non-shrub mean = 8% +/- 349, $p_{MW} < 0.01$; Figure 4g). Shrub and non-shrub transects were not statistically different in terms of changes in beach width ($p_{MW} = 0.10$; Figure 4h).

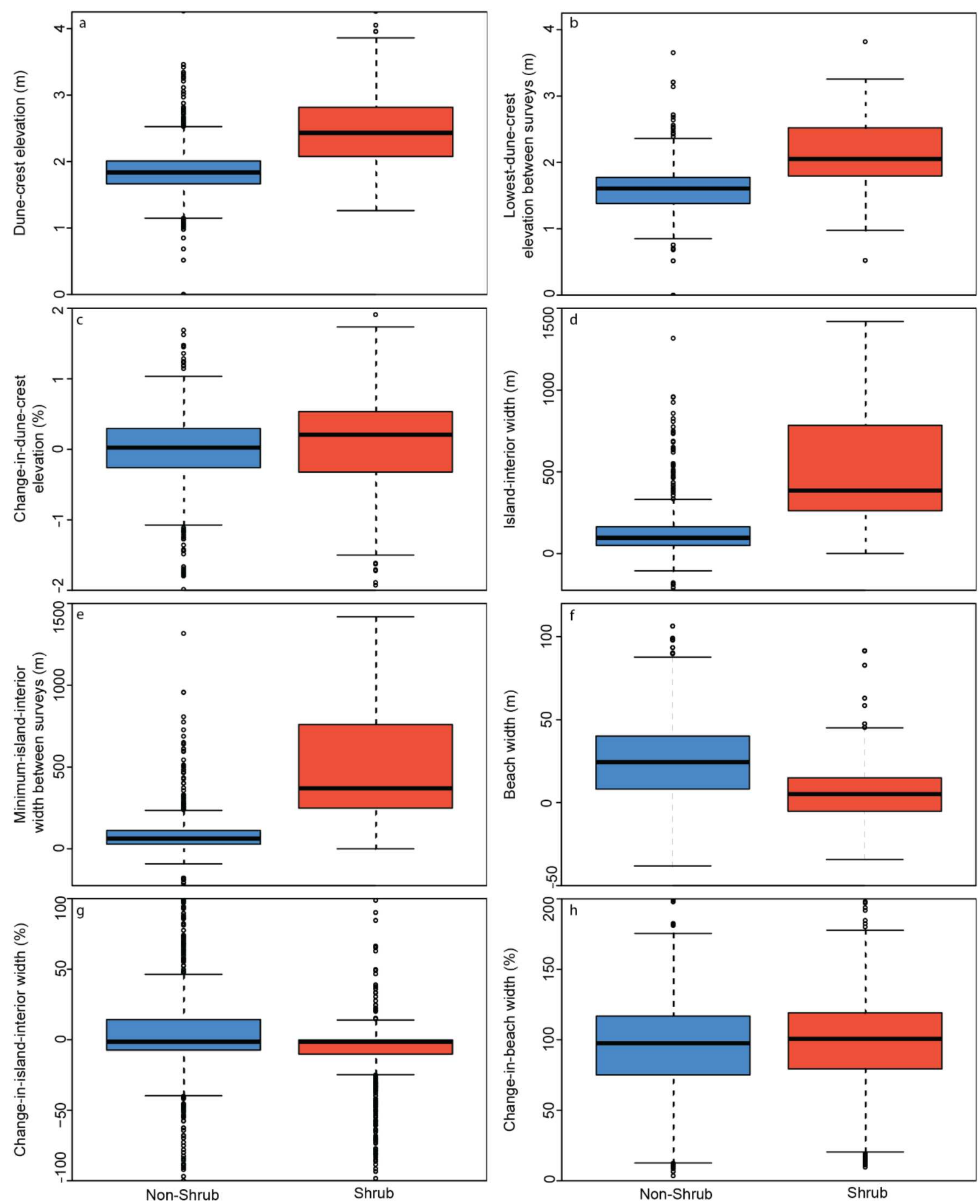

Figure 4. Summary of morphometric variables. Box and whisker plots showing non-shrub and shrub values for eight morphometric variables including: dune-crest elevation (a), lowest-dune-crest elevation between surveys (b), change-in-dune elevation (c), island-interior width (d), minimum-island-interior width between surveys (e), beach width (f), change-in-island-interior width (g), and change-in-beach width (h).

3.2 Decision Tree Predictions

The decision tree (Figure 5) grouped transects into four categories based on a combination of values for minimum-island-interior width between surveys and dune-crest elevation, resulting in predictions that are 90% accurate for the presence or absence of shrubs (Table 3). We found no statistically significant linear or polynomial correlation between dune-crest elevation and minimum-island-interior width between surveys, with multiple R-squared values below 0.3 (Figure 6). A summary of the four categories generated by the decision tree is presented in Table 4. The spatial extent of each category within the VCR is shown in Figure 7, and the values for dune-crest elevation and minimum-island-interior width between surveys that delineate the categories are indicated in Figure 6.

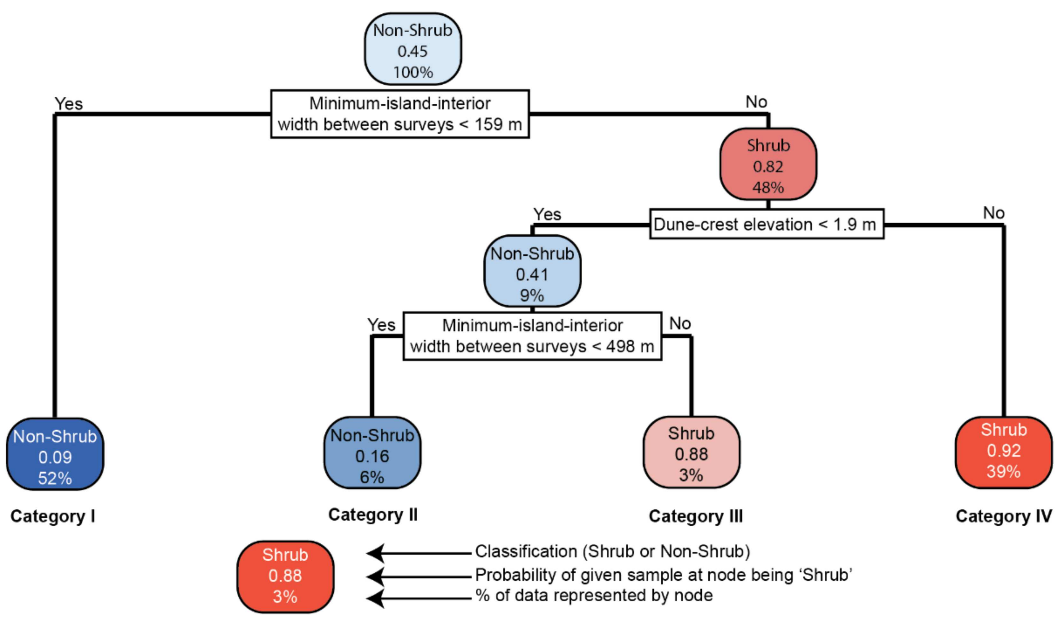

Figure 5. Shrub identification decision tree. Generated decision tree that makes predictions based on transect dune-crest elevation and minimum-island-interior width between surveys.

Table 3. Confusion matrices from decision tree (DT) and random forest (RF) predictions for both training and validation datasets.

DT Training Data (75%)	Observed Non-Shrub	Observed Shrub	DT Validation Data (25%)	Observed Non-Shrub	Observed Shrub
Predicted Non-Shrub	594	76	**Predicted Non-Shrub**	203	15

Predicted Shrub	53	441	**Predicted Shrub**	12	157
DT Accuracy		89%			93%
RF Training Data (75%)	**Observed Non-Shrub**	**Observed Shrub**	**RF Validation Data (25%)**	**Observed Non-Shrub**	**Observed Shrub**
Predicted Non-Shrub	607	40	**Predicted Non-Shrub**	203	26
Predicted Shrub	53	464	**Predicted Shrub**	12	146
RF Accuracy		92%			90%

Table 4. Summary of four categories generated from decision tree analysis.

Category	I	II	III	IV
% of Total Data	51.9%	5.7%	3.4%	39%
# of Transects	805	88	56	605
% Shrub	9%	16%	88%	92%
Dune-crest elevation	NA	> 1.9 m	> 1.9 m	< 1.9 m
Minimum-island-interior width between surveys	> ~ 160 m	~160 – ~500 m	< ~500 m	< ~ 160 m
Location within VCR	Northern half of Smith Island, Myrtle Island, Ship Shoal, the northern and southern thirds of Wreck Island, the southern half of Cobb Island (2010, 2016), the majority of Cobb Island (2017), the southern half of Parramore Island, and the northern half of Cedar Island	Cobb Island, the southern half of Parramore Island, and the southern third of Cedar Island	Southern quarter of Smith Island (2017), the northern third of Hog Island (2010), and the northern half of Parramore Island (2010, 2017)	Southern end of Smith, the middle third of Wreck Island, southern two-thirds of Hog Island (2010), all of Hog Island (2016 and 2017), the middle portion of Cobb (2010, 2016) Island, the northern half of Parramore Island, and the southern half of Cedar Island
Summary	Category I represents the largest category, had the lowest shrub percentage, and possessed the narrowest IIW$_{MBS}$ values	Category II had wider IIW$_{MBS}$ values compared to Category I, narrower IIW$_{MBS}$ values compared to Category III, and lower DCE's compared to Category IV	Category III had wider IIW$_{MBS}$ values compared to Categories I and II, and lower DCE measures than Category IV	Category had the majority of total shrub transects (79%), wider IIW$_{MBS}$ values compared to Categories I and II and higher DCE values compared to Categories II and III

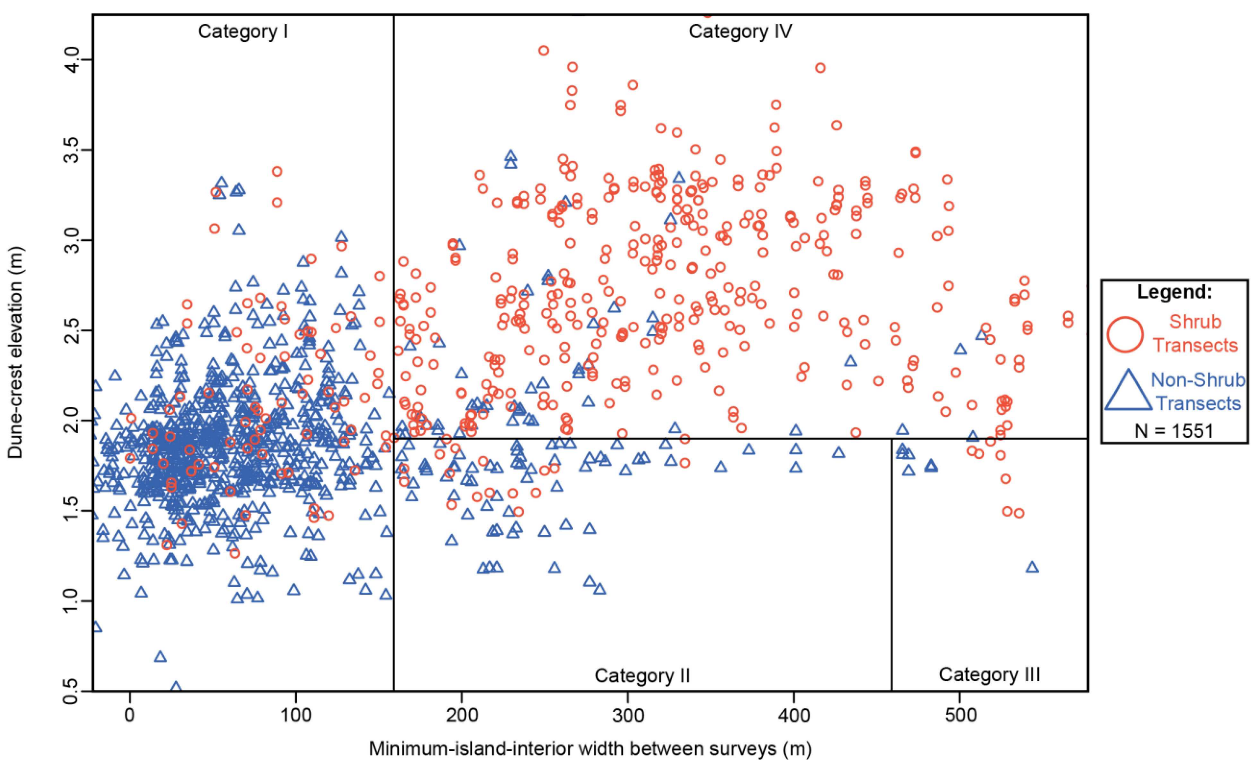

Figure 6. Dune-crest elevation versus minimum-island-interior width between surveys. Scatterplot showing dune-crest elevation versus minimum-island-interior width between surveys for shrub and non-shrub transects. Solid black lines show four categories generated by DT analysis based on dune-crest elevation and minimum-island-interior width between surveys.

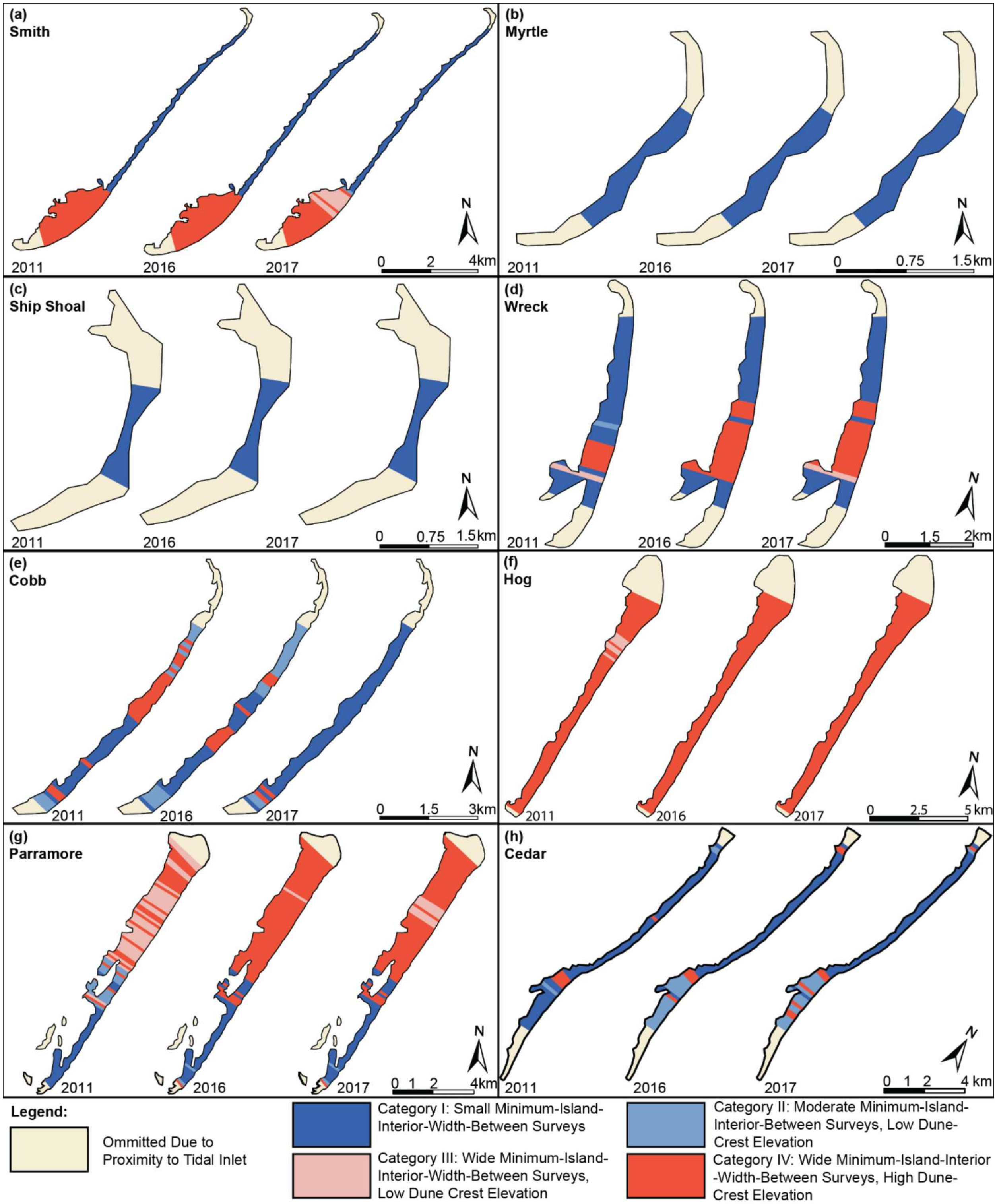

Figure 7. Decision tree categories by island over time. VCR islands color-coded according to decision tree categories for 2011, 2016, and 2017 composites for all eight islands: Smith (a), Myrtle (b), Ship Shoal (c), Wreck (d), Cobb (e), Hog (f), Parramore (g), and Cedar (h).

3.2.5 Misidentification

Focusing on the 10% of transects that were incorrectly categorized by the decision tree analysis, we found that misclassification due to hysteresis was the most common error representing 48% of total misidentifications (75 transects, 4.8% of total transects; Table 5). Remote sensing misidentification was the second largest error source, accounting for 28% of all errors (44 transects, 2.8% of total transects; Table 5), being most common where shrubs were less well established and had smaller spatial extents. We attributed the remaining 24% of error (36 transects, 2.4% of total transects, Table 5) to decision tree error, representing outlier data points, errors stemming from the DT method, and other assorted error sources not represented by hysteresis, remote sensing error, or the DT method.

Table 5. Summary statistics for misidentified transects by error type. The number of incorrectly identified transects associated with each type of error, as well as the percentage of transects within each type relative to the total number of misidentified transects and all transects studied.

Type of Error	Number of Transects (N)	% of Misidentifed transects	% of Transects Studied
System Hysteresis	75	48	4.8
Remote Sensing	44	28	2.8
Decision Tree	36	24	2.4

3.3 Areas of Shrub Colonization and Removal for Comparison with DT Thresholds

During the study period 181 transects changed shrub classification: Shrubs newly appeared on 87 transects (hereafter referred to as shrub colonization transects) and shrubs were no longer present on 94 transects (hereafter referred to as shrub removal transects). Comparing the dune-crest elevation and minimum-island-interior width between survey values of shrub colonization and loss transects to the threshold values generated by the decision tree analysis provides a useful check on the decision tree analysis. We found 96% of shrub colonization transects (N = 84) had dune crest elevations above ~1.9 m, with the lowest dune crest elevation being 1.76 m. In contrast, only 22% of shrub removal transects (N = 21) had elevations greater than ~1.9 m. Examining minimum-island-interior width between survey values, we found 79% of shrub colonization transects (N = 75) had IIW_{MBS} values of at least ~160 m, with 90% (N = 81) having IIW_{MBS} values of at least 100 m. Whereas 72% of shrub removal transects (N=68) had IIW_{MBS} values of less than ~160 m. Considering both DCE and IIW_{MBS} together, 76% of shrub colonization transects (N = 66) exceeded both thresholds (IIW_{MBS} values >160 m and DCE values >1.9 m), and 94% of shrub removal transects (N = 6) fell below both thresholds (IIW_{MBS} <160 m and DCE <1.9).

3.4 Random Forest Model

The random forest model made predictions with 92% accuracy using the training data and 90% accuracy when applied to the validation data (Table 3). Similar to the results of decision tree analysis, in the random forest model, minimum-island-interior width between surveys, dune-crest elevation, and island-interior width, were the most important morphometric variables for making accurate predictions about shrub presence (Figure 8). Omitting the minimum-island-interior width between surveys variable resulted in a 15.0% mean decrease in algorithm accuracy, whereas excluding island-interior width or dune-crest elevation decreased accuracy by ~8.3% or 7.8% respectively. Lowest-dune-crest elevation between surveys and beach width were the 4th and 5th most important variables, with their omissions resulting in a 4.7% and 3.3% decrease in mean accuracy. The change over time variables (change-in-dune elevation, change-in-beach width, change-in-island interior width had the lowest impact on mean accuracy resulting in 2.0%, 1.6% and 1.4% decreases respectively. Based on the respective mean decrease in accuracy percentages we see a significant spread in the importance of the different variables, with the most important variable being ~ 9 times more important than the least important variable and twice as important as the next most important variable (island-interior width). The change over time variables don't add much to the overall accuracy of the model. It is possible that the change values would be more important if the landcover changes could be measured over shorter time periods and at a higher spatial resolution than our data sources allow.

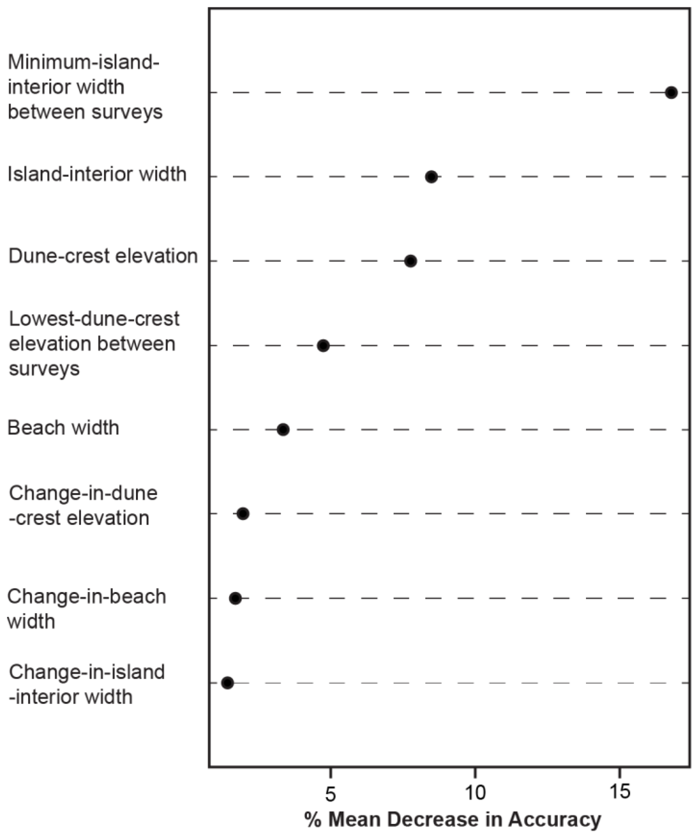

Figure 8. Random-forest variable importance plot. Plot shows the relative importance of the eight explanatory variables on RF model accuracy as measured by the percent decrease in accuracy arising from omitting the variable.

4 Discussion

4.1 Role of Minimum-Island-Interior Width Between Surveys and Dune-Crest Elevation

The decision tree resulting from our analysis accurately predicts the presence or absence of shrubs within the VCR based on the minimum-island-interior width between surveys and dune-crest elevation, with the former being most important. This is likely because minimum-island-interior width between surveys represents two important factors that affect shrub presence:

physical space and distance from saline island edges. Generally, relative to narrower islands, wider islands will have larger areas of potential shrub habitat, making it more likely that shrubs will seed, grow, and become established. The minimum-island-interior width between surveys serves as a rough proxy for the area of potential shrub habitat maintained over the period of observation. This finding is consistent with other studies that report on factors associated with the presence of woody vegetation on barrier islands. For example, though Velasquez-Montoya et al. (2021) focused on the effects of storms on multiple barrier island landcover classes, their finding that shrubs tend to be located on wider island segments and landward of an oceanfront road fronted by a dune is consistent with our findings that island width (and dune height) are related to shrub presence. Enwright et al. (2019) analyzed landcover for a developed Gulf Coast barrier island and found that in this environment woody vegetation, which included both shrubs and trees, was only found in the island interior where there was sufficient space available. Critically, by considering multiple snapshots in time, our work indicates that minimum-island-interior width between surveys (which is an indication of island width over time) is more important than island-interior width at the time of survey, suggesting that the response of shrubs to the limiting effect of island interior width is not instantaneous; minimum width within the recent past (relative to shrub survey timing) is more important than wider widths achieved either in the more distant past or present.

The importance of island width revealed by our analyses is consistent with previous work related to shrub habitat suitability, which demonstrates that wider island interiors provide protection from excess salinity and access to necessary freshwater. Shrubs are damaged by excess salinity (e.g., Du & Hesp, 2020; Miller et al., 2008; Young et al., 1994; Zinnert et al., 2011), which commonly arises from salt spray associated with breaking waves (Du & Hesp,

2020) or saltwater delivered by overwash or inundation during storms (Miller et al., 2008; Woods et al., 2019). Wider islands provide the opportunity for shrubs to be located a greater distance from the ocean, reducing salt spray and overwash exposure. While salt spray and soil salinity are an important control on shrub presence, they are not the only controlling factor, as highlighted by soil salinity levels from the VCR. Sabo (2023), found mean total-chloride salinity values of 16.9 ppm (SD of 195.6, N = 195) for soils on Hog and Parramore islands within the dune and barrier island interiors. Young et al. (1994) calculated soil salinity levels in areas with *Morella cerifera* within the VCR, observing soil chloride levels of less than 500 parts per million (ppm), with 88% being below 50 ppm. When findings from Young et al., (1994) are applied to soil samples from Hog and Metompkin islands, 98% (N= 195) of soil samples had soil chloride values below the 500 ppm threshold, with 72% of soil samples having chloride values below 50 ppm (Sabo, 2023). Since the majority samples (72 %) had soil chloride values below 50 ppm with 98% of samples being below 500 ppm, we conclude that soil salinity is not the sole determining factor in shrub presence within the VCR, and unlikely to control the distribution of shrubs in island interiors.

In addition to their sensitivity to saline conditions, shrubs require sufficient fresh groundwater to exist (Young et al., 2011). Greater island widths and higher interior elevations (Bolyard et al., 1979; Hayden et al., 1995) are important controls on the availability of fresh groundwater, with wider islands having a larger area to store and collect freshwater. Additionally, wider islands have a larger area unaffected by back-barrier saline intrusion, which otherwise lowers shrub habitat suitability by increasing groundwater salinity in flooded areas (Young et al., 1994). Some of the same positive attributes provided by wider island interior widths are also provided by high foredune elevations. High dunes can protect shrubs from damaging salt spray (Miller et al., 2008; Woods et al., 2019), prevent harmful overwash events (e.g., Houser et al., 2018; Reeves et al., 2021; Sallenger, 2000), and increase the amount of island groundwater storage (Bolyard et al., 1979; Hayden et al., 1995).

The decision tree algorithm yields a minimum-island-interior width between surveys threshold of >160 m and dune-crest elevation threshold of >1.9 m as predictive of shrub presence. The latter represents a refinement on earlier observations by Woods et al. (2019) of 1.75 m, which was determined from a smaller sample size. Categorizing transects into groups based only on minimum-island-interior width between surveys values, allows for predictions that are 91% accurate for non-shrub transects but lower, at an accuracy of 82%, for shrub transects. Improving accuracy for shrub transects requires considering both minimum-island-interior width between surveys and dune-crest elevation thresholds; using both values improves shrub prediction accuracy to 92%.

While the empirical relationships represented by Categories II and III arise from much smaller sample sizes than Categories I and IV and so are not as well supported as Categories I and IV, the relationships they represent are conceptually consistent with what we would expect based on factors that influence shrub presence or absence. Islands with sufficient minimum-island-interior width between surveys (IIW_{MBS}>~160 m), but lower dune-crest elevations (DCE < 1.9 m) are unlikely to have shrubs, with exceptions typically either having extremely wide interior widths (Category III, IIW_{MBS} > ~500 m) or older beachfront shrubs, which are in the process of being removed by coastal erosion (Category II) (as identified in Zinnert et al. 2019). In contrast, transects having both adequate minimum-island-interior width between surveys (IIW_{MBS} > ~160 m) and dune-crest elevations (DCE > 1.9 m; Category IV) are highly likely to have shrubs: > 92% of transects that met these two criteria are shrub transects, similar to Miller et al.'s (2008) findings that distance to shore and dune elevation affect the success of shrub seedlings.

The importance of interior-island width and dune elevation in determining shrub presence/absence from our decision tree analysis is corroborated and supported by the variable importance rankings arising from our random forest modeling. Because the decision tree modeling yields not only predictions, but also thresholds that can be further evaluated, in the next section we discuss how the results of the decision tree analysis allow us to better understand where predictions diverge from observations.

4.2 Decision Tree Misidentification

While definitive standards have not been set regarding machine learning accuracy, the accuracy of 90% achieved by our approach compares favorably to other recently published studies (e.g., accuracy scores of 93% from Adam et al. (2014), 75% from Barbella et al. (2021), and 86% from Gómez et al. (2022)) and is significantly higher than the no information rate (i.e., weighted on probability only) of 55%. Even so, it is valuable and informative to understand why our decision tree model doesn't correctly predict the remaining 10% of the data. Below, we discuss the three sources of error we identified.

4.2.1 System Hysteresis

Our machine learning approach involved using contemporaneous relationships between variables to derive predictions; however, physical changes in the island landscape (island interior and dune elevation) can occur on different timescales than shrub dynamics, leading to a lag between predicted and observed shrub behavior and misclassification due to system hysteresis. Although changes in the landscape can occur on the scale of days, it takes a few years for shrub seedlings to take hold and grow sufficiently large to significantly alter sediment transport processes (Reeves et al., 2022); larger shrubs have a greater effect on overwash processes.

Within the VCR, shrub thickets are rapidly transitioning from grasslands due to warming climate, a phenomenon seen in many other coastal and non-coastal systems (Woods et al., 2020; Young et al., 1994; Zinnert et al., 2021). In addition to maintaining favorable physical conditions for shrub establishment, areas need to meet requisite biological preconditions including presence of seeds and potentially, sufficient grass cover (Woods et al., 2019). Similarly, shrub decline and removal are not instantaneous; it can take a few years to shrubs to die and wash away after conditions are no longer conducive for shrub growth as witnessed by gradual removal of shrubs from the southern end of Smith Island (Figure 9) and the middle portion of Hog Island. While a single storm might remove a protective foredune in front of a shrub, it can take time for shrubs to die off because species like *Morella cerifera* are resistant to episodic saline flooding (Tolliver et al., 1997; Young et al., 1995).

Hysteresis is a well-documented phenomenon found in other VCR habitats, including lagoonal seagrass beds and marshes (Broome et al., 1988; Carr et al., 2012; Da Silveira Lobo Sternberg, 2001; Denny & Benedetti-Cecchi, 2012), which exhibit similar lags in establishment and removal. Prior to the 1930's, the lagoons behind the VCR were home to rich seagrass communities. However, during the 1930's a wasting disease and increases in lagoon temperatures led to a severe seagrass die off (Rasmussen, 1977). While physical conditions (light, nutrients, etc.) were sufficient for seagrass growth, the lack of seeds prevented natural recovery. This idea was supported by the rapid seagrass growth that occurred following the large-scale planting of seedings (Orth et al., 2012). Marshes can also exhibit a similar lag in reestablishment, as it took three years for pioneer marsh species in La Grande marsh (France) to reestablish following the cleanup of the Amoco Cadiz Oil Spill (Seneca & Broome, 1982), and a Portuguese marsh still showed reduced marsh plant richness 10 years after inputs of mercury pollution ceased compared to nearby uncontaminated marshes (Válega et al., 2008). The lag in seagrass and marsh establishment is analogous to the delay in shrub colonization we observed along the southern tip of Hog Island (also noted by Woods et al., 2019).

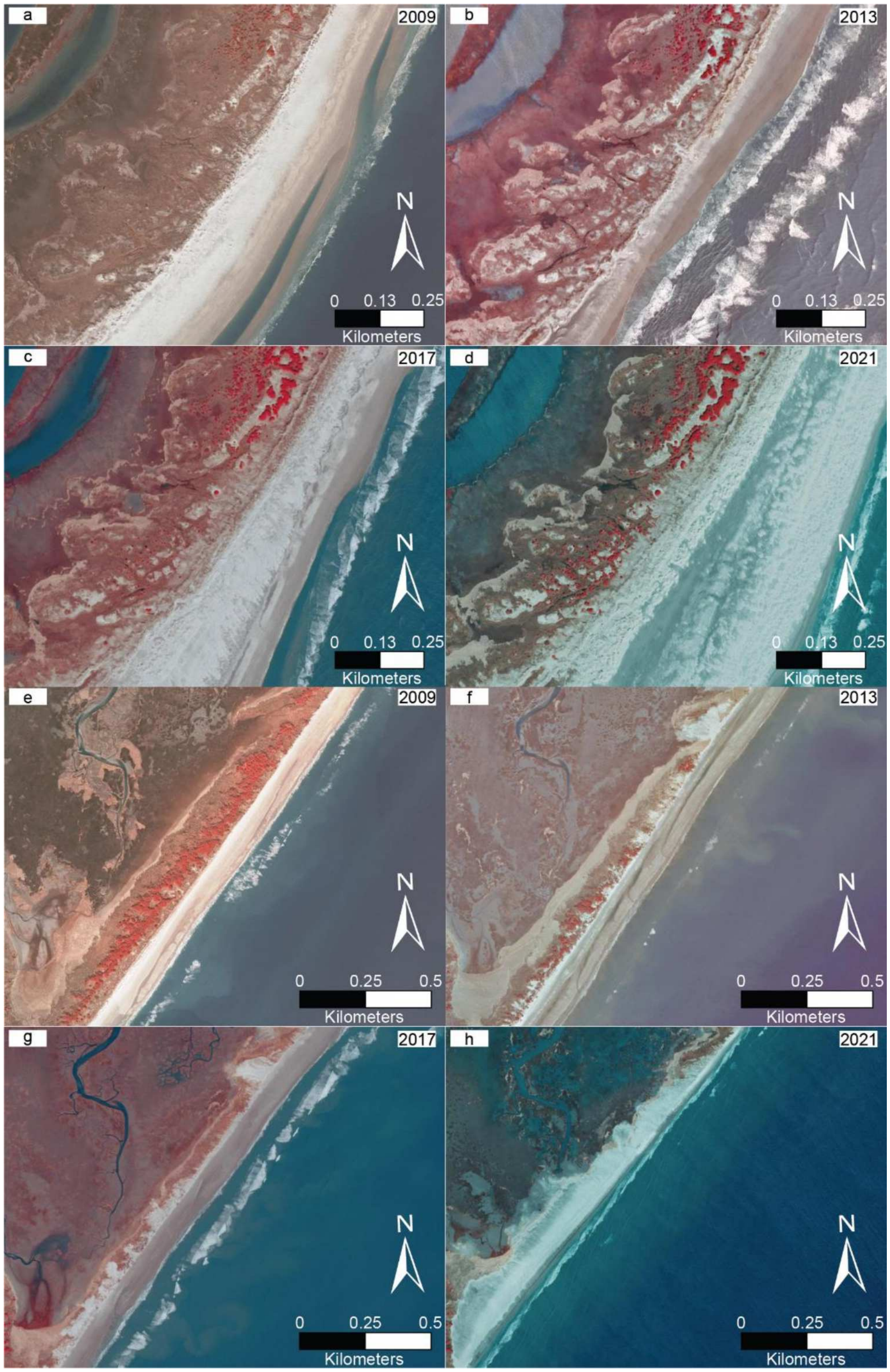

Figure 9. Examples of system hysteresis. Color-infrared aerial images (vegetation in red) showing (a-d) gradual shrub expansion on Hog Island in an area predicted to have shrubs but where observations revealed some transects had shrubs and some did not and (e-h) gradual removal of shrubs on Smith Island in an area predicted to be non-shrub but initially observed to have shrubs

In addition to displaying lagged behavior in establishment, seagrass, marsh, and shrubs show similar delayed patterns of system removal. Seagrass exhibits hysteresis when dying off and transitioning to bare sand, as it can take several years for seagrass to be removed when conditions are no longer conducive to seagrass presence (Carr et al., 2012), with the initial density of seagrass controlling the timeframe required to return to bare unvegetated sand. Marshes can temporally avoid drowning if fronted by a sufficiently large adjoining mudflat, under rates of relative sea-level rise and suspended sediment concentrations that do not support marsh persistence (Mariotti & Carr, 2014). Whereas the presence of wide mudflats may delay the inevitable, eventually these marshes will erode and drown as they equilibrate to new physical conditions (Mariotti & Carr, 2014). On the southern third of Smith Island (Figure 9 e-h), we observe a similar lag in shrub removal; based on our observations from aerial photography, it takes over 10 years for shrubs to be completely removed from an area.

A few examples highlight the lag between model predictions and shrub observations. Transects along the southern portion of Smith Island are consistently predicted to lack shrubs (consistent Category I designation). Although shrubs were initially present along this portion of Smith, shrub extent consistently decreased between 2009 and 2021 (Figure 9A-D), with most shrubs being removed by shoreline erosion between 2009 and 2013 (Figure 9e-f). By 2017, only a few isolated shrubs remained (Figure 9g), before they were completely removed by 2021 (Figure 9h). Similarly, the southern end of Hog Island was repeatedly predicted to have shrubs (Category IV). Despite this, shrubs were not initially present throughout, taking 10 years (2011-2021) to become established across all predicted areas (Figure 9a-d).

4.2.1.2 Shrub Colonization and Removal Transects

Our analysis of shrub colonization and shrub loss transects lends further support to the DCE and IIW_{MBS} threshold values associated with shrub presence and absence identified by the decision tree analysis. Measures of DCE are especially consistent, with 96% of shrub colonization transects having elevations above the 1.9 m DT threshold compared with only 16% of shrub removal transects. Focusing on IIW_{MBS} values, 79% of shrub colonization transects had widths exceeding the 160m DT threshold in contrast to 28% of shrub removal transects. Looking at DCE and IIW_{MBS} thresholds together, 76% of shrub colonization transects exceeded both threshold DT values, compared to just 6% of shrub removal transects, supporting the empirical relationships identified by the DT, as shrub presence is predicted based on having both high enough DCE and wide-enough IIW_{MBS}.

While applying DT thresholds to shrub colonization and removal data provides additional information that largely supports our DT analysis and thresholds, additional observations would be helpful to refine the specific IIW_{MBS} and DCE thresholds associated with shrub colonization or removal. While the DT analysis is adept at identifying the empirical thresholds associated with shrub presence or absence, it is less suited to predicting the specific thresholds at which an area will change from shrub to non-shrub because this method is based on correlations identified within the observations used in the analysis. Based on 96% of shrub colonization areas having elevations of at least 1.9 m, it seems practical to infer shrub colonization requires elevations of at least 1.9 m; while, the 79% of shrub growth transects with IIW_{MBS} values exceeding 160 m, provides validation for 160 m being a reasonable threshold to split the data, however the specific minimum width may be lower as 90% of transects had IIW_{MBS} values exceeding 100 m. Future field studies and LiDAR surveys could help us refine the specific IIW_{MBS} values associated with shrub colonization or removal.

4.2.2 Remote Sensing Misidentification

The remaining fourth island (Ship Shoal) does not display hysteresis, instead misclassification of transects on Ship Shoal arises from the misidentification of shrubs on LANDSAT imagery (Figure 10), highlighting a drawback of relying on LANDSAT data for small spatial and temporal scale analyses. Though, we note that while large LANDSAT-derived datasets will occasionally yield some misidentifications, the positive benefits derived from the large spatial and temporal scale of this type of data outweigh the potential detriment of occasional misidentifications. Empirically derived predictions such as those generated by machine learning have the potential to improve quality control on future data products derived from remotely sensed imagery, such as LANDSAT or LiDAR. The continued improvement in resolution and availability of LiDAR and satellite imagery will further improve the utility of remote sensing products for identifying barrier island landcover change.

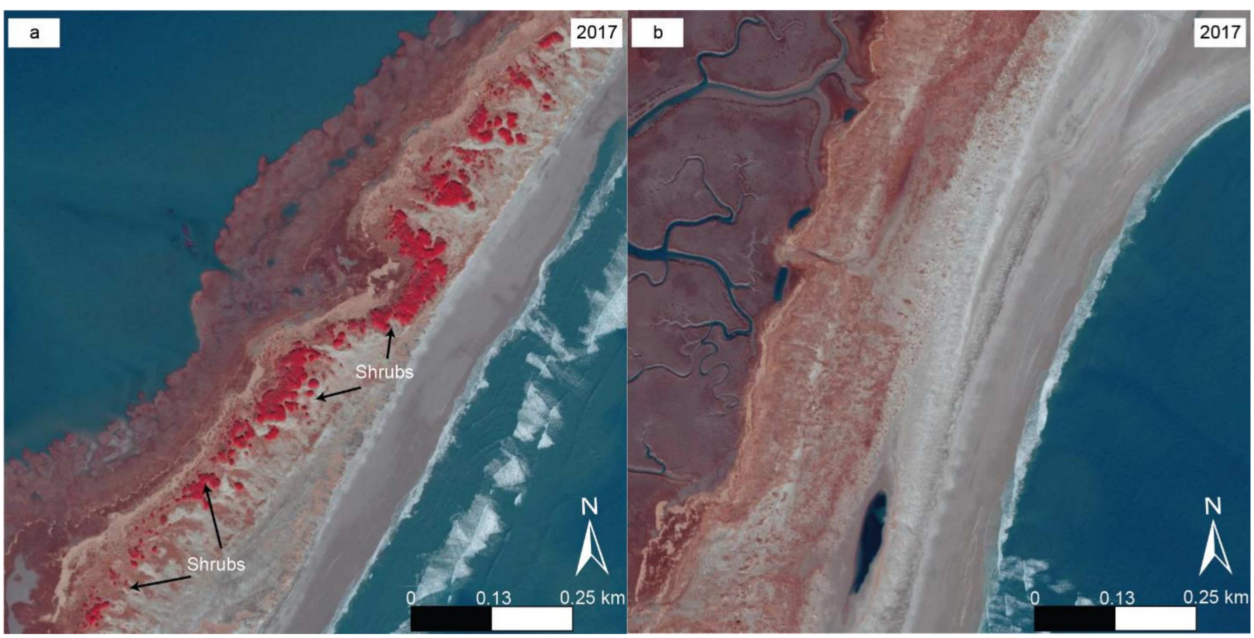

Figure 10. An illustrative example of remote sensing misidentification. Color-infrared aerial imagery (a) of Cobb Island, illustrating the typical appearance of shrubs for reference, for comparison with (b) imagery of Ship Shoal from an area that was incorrectly identified as having shrubs based on LANDSAT imagery.

4.2.3 Decision Tree Misidentification

The remaining misclassified transects cannot be attributed to hysteresis or remote sensing errors and thus represent outlier data points that may arise from the misidentification of certain dune, beach, or island interior properties. The existence of decision tree misclassification within our data, highlights that no empirical relationship will ever be 100% accurate, as nature rarely falls entirely into neat categories; however, the small number of algorithm-based errors supports the veracity of our derived empirical thresholds.

4.3 Potential Model Limitations, Applications and Future Work

Despite the potential applications of our approach and results, it is worth considering their limitations. Because of constraints arising from the availability of data, we studied a relatively short time period representing roughly 15 years. Extending this analysis over longer time periods may reveal different or altered empirical relationships or provide further support for the relationships we identify here. Conducting a similar analysis with new remote sensing data and identifying areas of continued match or mismatch between predicted and observed shrub behavior would allow quantification of the timescales associated with hysteresis in shrub colonization and removal. Additional data, potentially including field observations, may be most useful in refining and assessing the validity of the Category II and III classifications, which represent 10% of the data. Additionally, using LiDAR data, LANDSAT imagery and aerial imagery collected within the same month would be most ideal, but given the accuracy achieved by the models developed here using the data available, we anticipate that more synchronous timing of data sets would yield only minor improvements.

Although the new empirically derived relationships we identify have a high predictive accuracy for describing the VCR, when applying these relationships beyond the VCR it will be important to test them against data from other barrier island systems because landscape characteristics and woody vegetation extent may differ across varying barrier island types, climates, and vegetation species. Even within the VCR, climate change and the resulting large-scale alterations to the barrier island system may alter the applicability of the machine learning models to make correct predictions in the future, as observed empirical relationships could be different in a changing climate. Repeating our approach on future observations will allow assessment of whether or not the identified relationships and empirical thresholds remain the same or change.

While the relationships we identified are valid for the undeveloped VCR, they may be less applicable to developed coastal areas, where humans have a greater impact on species composition. For example, plantings, dune construction, nourishment and the presence of infrastructure alter island geomorphology, especially in the island interior behind dunes.

Applying a machine learning algorithm, such as the one developed here, to future predictions of dune and island morphometrics from geomorphic models, will allow prediction of future shrub presence/extent and absence, and assessment of whether or not shrub-overwash dynamics should be included in model runs (e.g., Reeves et al., 2022).

In addition to providing the potential for future assessments of shrub colonization and growth, and allowing assessment of the importance of including shrub dynamics within existing geomorphic models (Reeves et al., 2021, 2022), thresholds from decision tree models for predicted shrub colonization and removal could be coupled with, or integrated into, spatially explicit barrier island models, in a hybrid modeling approach. Hybrid approaches combine data-driven models with numerical models (Beuzen & Splinter, 2020; Goldstein & Coco, 2015), and their utility in the study of coastal environments continues to evolve and expand (e.g. Itzkin et al., 2022; Montaño et al., 2020). For example, Enwright et al. (2021) demonstrated the utility of employing a hybrid modeling approach to look at land-cover relationships to barrier island migration on the developed barrier Dauphin Island. Integrating machine learning algorithms trained with data from undeveloped systems, within geomorphic models that simulate barrier island evolution over time, would provide another means (in addition to Reeves et al., 2022) for shrub and barrier dynamics to evolve dynamically throughout model runs, potentially yielding further insights into the importance of ecomorphodynamic interactions in barrier response to changing conditions over decadal to centurial timescales.

5 Conclusions

Using machine learning, we identified empirical relationships between island geomorphology and shrubs that can accurately predict the presence of shrubs within the VCR. We find that minimum-island-interior width between surveys and dune-crest elevation are the most important variables for making accurate predictions, with minimum-island-interior width between surveys being sufficient to predict a lack of shrubs, while both minimum-island-interior width between surveys and dune-crest elevation are needed to predict shrub presence.

Islands with minimum-island-interior width between survey values less than ~160 m tend to lack shrubs (Category I), whereas areas that have dune-crest elevation values above 1.9 m and minimum-island-interior width between survey values exceeding ~160 m (Category IV) tend to have shrubs.

We attribute errors in our machine learning predictions to a combination of system hysteresis, remote sensing, and decision tree misclassification. Based on our analysis of misidentified transects, we find that shrub presence is a lagging indicator of change, with shrubs requiring time to adapt to changes in dune elevation or interior width that allow their growth. In the future, by looking at the areas where the observations diverge from model predictions, we can gain new insights into system evolution, the timescales of hysteresis, and improve future remote sensing classifications.

Acknowledgements

The authors acknowledge that there aren't any conflicts of interest in this research. This research was supported by the Virginia Coastal Reserve Long-Term Ecological Research Program (National Science Foundation DEB-1832221) via a subaward to Laura J. Moore at the University of North Carolina at Chapel Hill and Julie C. Zinnert at Virginia Commonwealth University and by the Preston Jones and Mary Elizabeth Frances Dean Martin Fellowship Fund from the Department of Earth, Marine, and Environmental Sciences at the University of North Carolina at Chapel Hill.

Open Research

All morphometric data and code used to generate this analysis is archived on Zendo (Franklin, 2024). Information to access DEMs of the Virginia Coastal Reserve are available in these in-text data citations (OCM Partners, 2023a, 2023a; VITA, 2018). Barrier island landcover can be accessed from the VCR data repository cited here (Zinnert, 2022). Aerial imagery are available from the Virginia Geographic Information Network's Virginia GIS Clearinghouse (Virginia

Geographic Information Network, 2009a, 2009b, 2013a, 2013b, 2017b, 2017a, 2021a, 2021b). Soil salinity data from VCR barrier islands is stored on the VCR data repository (Sabo & Zinnert, 2022).

References

Adam, E., Mutanga, O., Odindi, J., & Abdel-Rahman, E. M. (2014). Land-use/cover classification in a heterogeneous coastal landscape using RapidEye imagery: Evaluating the performance of random forest and support vector machines classifiers. *International Journal of Remote Sensing*, *35*(10), 3440–3458. https://doi.org/10.1080/01431161.2014.903435

Anderson, C. P., Carter, G. A., & Funderburk, W. R. (2016). The use of aerial RGB imagery and LIDAR in comparing ecological habitats and geomorphic features on a natural versus man-made barrier island. *Remote Sensing*, *8*(7), 602.

Ashton, A. D., & Lorenzo-Trueba, J. (2018). Morphodynamics of barrier response to sea-level rise. In L. J. Moore & A. B. Murray (Eds.), *Barrier Dynamics and Response to Changing Climate* (pp. 277–304). Springer International Publishing. https://doi.org/10.1007/978-3-319-68086-6_9

Barbarella, M., Di Benedetto, A., & Fiani, M. (2021). Application of supervised machine learning technique on LiDAR data for monitoring coastal land evolution. *Remote Sensing*, *13*(23), 4782. https://doi.org/10.3390/rs13234782

Beets, D. J., & van der Spek, A. J. (2000). The Holocene evolution of the barrier and the back-barrier basins of Belgium and the Netherlands as a function of late Weichselian morphology, relative sea-level rise and sediment supply. *Netherlands Journal of Geosciences*, *79*(1), 3–16.

Beuzen, T., & Splinter, K. (2020). Machine learning and coastal processes. In *Sandy Beach Morphodynamics* (pp. 689–710). Elsevier. https://doi.org/10.1016/B978-0-08-102927-5.00028-X

Bolyard, T. H., Hornberger, G. M., Dolan, R., & Hayden, B. P. (1979). Freshwater reserves of mid-atlantic coast barrier Islands. *Environmental Geology*, *3*(1), 1–11. https://doi.org/10.1007/BF02423273

Breiman, L. (2001). Random forests. *Machine Learning*, *45*, 5–32.

Breiman, L., Friedman, J. H., Olshen, R. A., & Stone, C. J. (1984). *Classification and regression trees*. Chapman & Hall.

Broome, S. W., Seneca, E. D., & Woodhouse, W. W. (1988). Tidal salt marsh restoration. *Aquatic Botany*, *32*(1–2), 1–22. https://doi.org/10.1016/0304-3770(88)90085-X

Carr, J. A., D'Odorico, P., McGlathery, K. J., & Wiberg, P. L. (2012). Stability and resilience of seagrass meadows to seasonal and interannual dynamics and environmental stress. *Journal of Geophysical Research: Biogeosciences*, *117*(G1). https://doi.org/10.1029/2011JG001744

Carter, G. A., Otvos, E. G., Anderson, C. P., Funderburk, W. R., & Lucas, K. L. (2018). Catastrophic storm impact and gradual recovery on the Mississippi-Alabama barrier islands, 2005–2010: Changes in vegetated and total land area, and relationships of post-storm ecological communities with surface elevation. *Geomorphology*, *321*, 72–86. https://doi.org/10.1016/j.geomorph.2018.08.020

Ciarletta, D. J., Lorenzo-Trueba, J., & Ashton, A. D. (2019). Mechanism for retreating barriers to autogenically form periodic deposits on continental shelves. *Geology*, *47*(3), 239–242. https://doi.org/10.1130/G45519.1

Cipriani, L. E., & Stone, G. W. (2001). Net longshore sediment transport and textural changes in beach sediments along the southwest Alabama and Mississippi barrier islands, USA. *Journal of Coastal Research*, 443–458.

Da Silveira Lobo Sternberg, L. (2001). Savanna-forest hysteresis in the tropics: *Savanna-forest hysteresis*. *Global Ecology and Biogeography*, *10*(4), 369–378. https://doi.org/10.1046/j.1466-822X.2001.00243.x

De'ath, G., & Fabricius, K. E. (2000). Classification and regression trees: A powerful yet simple technique for ecological data analysis. *Ecology*, *81*(11), 3178–3192. https://doi.org/10.1890/0012-9658(2000)081[3178:CARTAP]2.0.CO;2

Denny, M., & Benedetti-Cecchi, L. (2012). Scaling up in ecology: Mechanistic approaches. *Annual Review of Ecology, Evolution, and Systematics*, *43*(1), 1–22. https://doi.org/10.1146/annurev-ecolsys-102710-145103

Donnelly, C., Kraus, N., & Larson, M. (2006). State of knowledge on measurement and modeling of coastal overwash. *Journal of Coastal Research*, *22*(4), 965–991.

Du, J., & Hesp, P. A. (2020). Salt Spray Distribution and Its Impact on Vegetation Zonation on Coastal Dunes: A Review. *Estuaries and Coasts*, *43*(8), 1885–1907. https://doi.org/10.1007/s12237-020-00820-2

Duncan, W. H., & Duncan, M. B. (1987). *The Smithsonian guide to seaside plants of the Gulf and Atlantic coasts* (1st ed.). Smithsonian Institution Press.

Durán Vinent, O., & Moore, L. J. (2015). Barrier island bistability induced by biophysical interactions. *Nature Climate Change*, *5*(2), 158–162.

Ehrenfeld, J. G. (1990). Dynamics and processes of barrier-island vegetation. *Reviews in Aquatic Sciences*, *2*(3–4), 437–480.

Enwright, N. M., Wang, L., Borchert, S. M., Day, R. H., Feher, L. C., & Osland, M. J. (2019). Advancing barrier island habitat mapping using landscape position information. *Progress in Physical Geography: Earth and Environment*, *43*(3), 425–450. https://doi.org/10.1177/0309133319839922

Enwright, N. M., Wang, L., Dalyander, P. S., Wang, H., Osland, M. J., Mickey, R. C., Jenkins, R. L., & Godsey, E. S. (2021). Assessing Habitat Change and Migration of Barrier Islands. *Estuaries and Coasts*, *44*(8), 2073–2086. https://doi.org/10.1007/s12237-021-00971-w

Fisher, K. R., Ewing, R. C., & Duran Vinent, O. (2023). Decadal and seasonal changes in landcover at Padre Island: Implications for the role of the back-barrier in signaling island state change. *Earth Surface Processes and Landforms*, *48*(1), 163–178. https://doi.org/10.1002/esp.5479

Fitzgerald, D. M., Penland, S., & Nummedal, D. A. G. (1984). Control of barrier island shape by inlet sediment bypassing: East Frisian Islands, West Germany. *Marine Geology*, *60*(1–4), 355–376.

Franklin, B. (2024). *franklin1895/Predicting_Barrier_Island_Shrub_Presence: Code & Data Repository* (v1.1) [Computer software]. Zenodo. https://doi.org/10.5281/zenodo.10806356

Goldstein, E. B., & Coco, G. (2015). Machine learning components in deterministic models: Hybrid synergy in the age of data. *Frontiers in Environmental Science*, *3*. https://doi.org/10.3389/fenvs.2015.00033

Goldstein, E. B., Coco, G., & Murray, A. B. (2013). Prediction of wave ripple characteristics using genetic programming. *Continental Shelf Research*, *71*, 1–15. https://doi.org/10.1016/j.csr.2013.09.020

Goldstein, E. B., Coco, G., & Plant, N. G. (2019). A review of machine learning applications to coastal sediment transport and morphodynamics. *Earth-Science Reviews*, *194*, 97–108. https://doi.org/10.1016/j.earscirev.2019.04.022

Gómez, R. D., Pasternack, G. B., Guillon, H., Byrne, C. F., Schwindt, S., Larrieu, K. G., & Solis, S. S. (2022). Mapping subaerial sand-gravel-cobble fluvial sediment facies using airborne lidar and machine learning. *Geomorphology*, *401*, 108106.

Hastie, T., Tibshirani, R., Friedman, J. H., & Friedman, J. H. (2009). *The elements of statistical learning: Data mining, inference, and prediction* (Vol. 2). Springer.

Hayden, B. P., Santos, M. C., Shao, G., & Kochel, R. C. (1995). Geomorphological controls on coastal vegetation at the Virginia Coast Reserve. *Geomorphology*, *13*(1–4), 283–300.

Houser, C., Lehner, J., & Smith, A. (2022). The field geomorphologist in a time of artificial intelligence and machine learning. *Annals of the American Association of Geographers*, *112*(5), 1260–1277. https://doi.org/10.1080/24694452.2021.1985956

Houser, C., Wernette, P., & Weymer, B. A. (2018). Scale-dependent behavior of the foredune: Implications for barrier island response to storms and sea-level rise. *Geomorphology*, *303*, 362–374.

Huang, H., Zinnert, J. C., Wood, L. K., Young, D. R., & D’Odorico, P. (2018). Non-linear shift from grassland to shrubland in temperate barrier islands. *Ecology*, *99*(7), 1671–1681.

Inman, D. L., & Dolan, R. (1989). The Outer Banks of North Carolina: Budget of sediment and inlet dynamics along a migrating barrier system. *Journal of Coastal Research*, 193–237.

Itzkin, M., Moore, L. J., Ruggiero, P., & Hacker, S. D. (2020). The effect of sand fencing on the morphology of natural dune systems. *Geomorphology*, *352*, 106995. https://doi.org/10.1016/j.geomorph.2019.106995

Itzkin, M., Moore, L. J., Ruggiero, P., Hovenga, P. A., & Hacker, S. D. (2022). Combining process-based and data-driven approaches to forecast beach and dune change. *Environmental Modelling & Software*, *153*, 105404.

Lary, D. J., Alavi, A. H., Gandomi, A. H., & Walker, A. L. (2016). Machine learning in geosciences and remote sensing. *Geoscience Frontiers*, *7*(1), 3–10. https://doi.org/10.1016/j.gsf.2015.07.003

Leatherman, S. P. (1983). Barrier dynamics and landward migration with Holocene sea-level rise. *Nature*, *301*(5899), 415–417. https://doi.org/10.1038/301415a0

Leatherman, S. P., Geological Society of America, & Society of Economic Paleontologists and Mineralogists (Eds.). (1979). *Barrier islands from the Gulf of St. Lawrence to the Gulf of Mexico*. Academic Press.

Liaw, A., & Wiener, M. (2022). *RandomForest: Breiman and Cutler’s random forests for classification and regression* (4.7-1.1) [Computer software]. https://cran.r-project.org/web/packages/randomForest/index.html

Lorenzo-Trueba, J., & Ashton, A. D. (2014). Rollover, drowning, and discontinuous retreat: Distinct modes of barrier response to sea-level rise arising from a simple morphodynamic model. *Journal of Geophysical Research: Earth Surface*, *119*(4), 779–801.

Luan, J., Zhang, C., Xu, B., Xue, Y., & Ren, Y. (2020). The predictive performances of random forest models with limited sample size and different species traits. *Fisheries Research*, *227*, 105534.

Mariotti, G., & Carr, J. (2014). Dual role of salt marsh retreat: Long-term loss and short-term resilience. *Water Resources Research*, *50*(4), 2963–2974. https://doi.org/10.1002/2013WR014676

Mariotti, G., & Hein, C. J. (2022). Lag in response of coastal barrier-island retreat to sea-level rise. *Nature Geoscience*, *15*(8), 633–638. https://doi.org/10.1038/s41561-022-00980-9

Martínez Prentice, R., Villoslada Peciña, M., Ward, R. D., Bergamo, T. F., Joyce, C. B., & Sepp, K. (2021). Machine Learning Classification and Accuracy Assessment from High-Resolution Images of Coastal Wetlands. *Remote Sensing*, *13*(18), Article 18. https://doi.org/10.3390/rs13183669

Maxwell, A. E., Warner, T. A., & Fang, F. (2018). Implementation of machine-learning classification in remote sensing: An applied review. *International Journal of Remote Sensing*, *39*(9), 2784–2817. https://doi.org/10.1080/01431161.2018.1433343

McAllister, E., Payo, A., Novellino, A., Dolphin, T., & Medina-Lopez, E. (2022). Multispectral satellite imagery and machine learning for the extraction of shoreline indicators. *Coastal Engineering*, *174*, 104102. https://doi.org/10.1016/j.coastaleng.2022.104102

Miller, D. L., Thetford, M., & Schneider, M. (2008). Distance from the Gulf influences survival and growth of three barrier island dune plants. *Journal of Coastal Research*, *4*, 261–266. https://doi.org/10.2112/07-0914.1

Montaño, J., Coco, G., Antolínez, J. A., Beuzen, T., Bryan, K. R., Cagigal, L., Castelle, B., Davidson, M. A., Goldstein, E. B., & Ibaceta, R. (2020). Blind testing of shoreline evolution models. *Scientific Reports*, *10*(1), 2137.

Moore, L. J., List, J. H., Williams, S. J., & Stolper, D. (2010). Complexities in barrier island response to sea level rise: Insights from numerical model experiments, North Carolina Outer Banks. *Journal of Geophysical Research: Earth Surface*, *115*(F3).

Morgan, J., Daugherty, R., Hilchie, A., & Carey, B. (2003). *Sample size and modeling accuracy of decision tree based data mining tools*. *6*(2).

Morton, R. A., & Sallenger Jr, A. H. (2003). Morphological impacts of extreme storms on sandy beaches and barriers. *Journal of Coastal Research*, 560–573.

Mull, J., & Ruggiero, P. (2014). Estimating storm-induced dune erosion and overtopping along US West Coast beaches. *Journal of Coastal Research*, *30*(6), 1173–1187.

Nienhuis, J. H., & Lorenzo-Trueba, J. (2019). Can barrier islands survive sea-level rise? Quantifying the relative role of tidal inlets and overwash deposition. *Geophysical Research Letters*, *46*(24), 14613–14621.

OCM Partners. (2023a). *2016 USACE Post-Matthew topobathy lidar DEM: Southeast Coast (VA, NC, SC, GA and FL)* [dataset]. https://www.fisheries.noaa.gov/inport/item/49409

OCM Partners. (2023b). *2017 USACE NCMP topobathy lidar DEM: East Coast (NY, NJ, DE, MD, VA, NC, SC, GA)* [dataset]. https://www.fisheries.noaa.gov/inport/item/52446

Orth, R., Moore, K., Marion, S., Wilcox, D., & Parrish, D. (2012). Seed addition facilitates eelgrass recovery in a coastal bay system. *Marine Ecology Progress Series*, *448*, 177–195. https://doi.org/10.3354/meps09522

Oshiro, T. M., Perez, P. S., & Baranauskas, J. A. (2012). How many trees in a random forest? *Machine Learning and Data Mining in Pattern Recognition: 8th International Conference, MLDM 2012, Berlin, Germany, July 13-20, 2012. Proceedings 8*, 154–168.

Oster, D., & Moore, L. (2019). *Beach Morphology of the Virginia Barrier Islands 1998, 2005 and 2009* [dataset]. Environmental Data Initiative. https://doi.org/10.6073/PASTA/09C14D85B004205DE6F558854941671A

Perry, G. L. W., & Dickson, M. E. (2018). Using machine learning to predict geomorphic disturbance: The effects of sample size, sample prevalence, and sampling strategy. *Journal of Geophysical Research: Earth Surface*, *123*(11), 2954–2970. https://doi.org/10.1029/2018JF004640

Rasmussen, E. (1977). The wasting disease of eelgrass (Zostera marina) and its effects on environmental factors and fauna. *Seagrass Ecosystems*, 1–51.

Reeves, I. R. B., Goldstein, E. B., Moore, L. J., & Zinnert, J. C. (2022). Exploring the impacts of shrub-overwash feedbacks in coastal barrier systems with an ecological-morphological model. *Journal of Geophysical Research: Earth Surface*, *127*(3). https://doi.org/10.1029/2021JF006397

Reeves, I. R. B., Moore, L. J., Murray, A. B., Anarde, K. A., & Goldstein, E. B. (2021). Dune dynamics drive discontinuous barrier retreat. *Geophysical Research Letters*, *48*(13), e2021GL092958. https://doi.org/10.1029/2021GL092958

Robbins, M. G., Shawler, J. L., & Hein, C. J. (2022). Contribution of longshore sand exchanges to mesoscale barrier-island behavior: Insights from the Virginia Barrier Islands, US East Coast. *Geomorphology*, *403*, 108163.

Sabo, A. (2023). Dune building dynamics impact cross-island connectivity and barrier island characteristics. *VCU Theses and Dissertations*. https://doi.org/10.25772/NG7M-G291

Sabo, A., & Zinnert, J. C. (2022). *Barrier Island Plant and Soil Properties on Hog and Metompkin Islands, Virginia, 2021-2022* (knb-lter-vcr.392.2) [dataset]. Environmental Data Initiative. https://www.vcrlter.virginia.edu/cgi-bin/showDataset.cgi?docid=knb-lter-vcr.392

Sallenger Jr, A. H. (2000). Storm impact scale for barrier islands. *Journal of Coastal Research*, 890–895.

Seneca, E. D., & Broome, S. W. (1982). Restoration of marsh vegetation impacted by the Amoco Cadiz oil spill and subsequent clean up operations at lle Grande France. *Ecological Studies of the Amoco Cadiz Oil Spill. Report of the NOAA-CNEXO Joint Scientific Commission, CNEXO, Paris*, 363–419.

Shiflett, S. A., & Young, D. R. (2010). Avian seed dispersal on Virginia Barrier Islands: Potential influence on vegetation community structure and patch dynamics. *The American Midland Naturalist*, *164*(1), 91–106. https://doi.org/10.1674/0003-0031-164.1.91

Snyder, R. A., & Boss, C. L. (2002). Recovery and stability in barrier island plant communities. *Journal of Coastal Research*, 530–536.

Stutz, M. L., & Pilkey, O. H. (2011). Open-ocean barrier islands: Global influence of climatic, oceanographic, and depositional settings. *Journal of Coastal Research*, *27*(2), 207–222.

Therneau, T., Atkinson, B., port, B. R. (producer of the initial R., & maintainer 1999-2017). (2022). *Rpart: Recursive partitioning and regression trees* (4.1.19) [Computer software]. https://cran.r-project.org/web/packages/rpart/index.html

Tolliver, K. S., Martin, D. W., & Young, D. R. (1997). Freshwater and saltwater flooding response for woody species common to barrier island swales. *Wetlands*, *17*(1), 10–18. https://doi.org/10.1007/BF03160714

Válega, M., Lillebø, A. I., Pereira, M. E., Duarte, A. C., & Pardal, M. A. (2008). Long-term effects of mercury in a salt marsh: Hysteresis in the distribution of vegetation following recovery from contamination. *Chemosphere*, *71*(4), 765–772. https://doi.org/10.1016/j.chemosphere.2007.10.013

Velasquez-Montoya, L., Sciaudone, E. J., Harrison, R. B., & Overton, M. (2021). Land cover changes on a barrier island: Yearly changes, storm effects, and recovery periods. *Applied Geography*, *135*, 102557.

Virginia Geographic Information Network. (2009a). *VBMP 2009 infrared WGS Web Mercator (VGIN)* [dataset]. https://vgin.vdem.virginia.gov/pages/clearinghouse

Virginia Geographic Information Network. (2009b). *VBMP 2009 WGS Web Mercator (VGIN)* [dataset]. https://vgin.vdem.virginia.gov/datasets/VGIN::vbmp-2009-wgs-web-mercator-vgin/about

Virginia Geographic Information Network. (2013a). *VBMP 2013 infrared WGS Web Mercator (VGIN)* [dataset]. https://vgin.vdem.virginia.gov/datasets/VGIN::vbmp-2013-infrared-wgs-web-mercator-vgin/about

Virginia Geographic Information Network. (2013b). *VBMP 2013 WGS Web Mercator (VGIN)* [dataset]. https://vgin.vdem.virginia.gov/datasets/VGIN::vbmp-2013-wgs-web-mercator-vgin/about

Virginia Geographic Information Network. (2017a). *VBMP 2017 infrared WGS Web Mercator (VGIN)* [dataset]. https://vgin.vdem.virginia.gov/datasets/VGIN::vbmp-2017-infrared-wgs-web-mercator-vgin/about

Virginia Geographic Information Network. (2017b). *VBMP 2017 WGS Web Mercator (VGIN)* [dataset]. https://vgin.vdem.virginia.gov/datasets/VGIN::vbmp-2017-wgs-web-mercator-vgin/about

Virginia Geographic Information Network. (2021a). *VBMP 2021 infared WGS Web Mercator (VGIN)* [dataset]. https://vgin.vdem.virginia.gov/pages/clearinghouse

Virginia Geographic Information Network. (2021b). *VBMP 2021 WGS Web Mercator (VGIN)* [dataset]. https://vgin.vdem.virginia.gov/datasets/VGIN::vbmp-2021-wgs-web-mercator-vgin/about

VITA. (2018). *LiDAR-based Digital Elevation Model for Northampton and Accomack Co., VA, 2010* [dataset]. Environmental Data Initiative. https://doi.org/10.6073/PASTA/EF88A4D75F9924B27D095D1FED91078C

Williams, J. R., Dellapenna, T. M., & Lee, G. (2013). Shifts in depositional environments as a natural response to anthropogenic alterations: Nakdong Estuary, South Korea. *Marine Geology*, *343*, 47–61.

Wood, L. K., Hays, S., & Zinnert, J. C. (2020). Decreased temperature variance associated with biotic composition enhances coastal shrub encroachment. *Scientific Reports*, *10*(1), 8210.

Woods, N. N., Dows, B. L., Goldstein, E. B., Moore, L. J., Young, D. R., & Zinnert, J. C. (2019). Interaction of seed dispersal and environmental filtering affects woody encroachment patterns in coastal grassland. *Ecosphere*, *10*(7). https://doi.org/10.1002/ecs2.2818

Young, D. R., Brantley, S. T., Zinnert, J. C., & Vick, J. K. (2011). Landscape position and habitat polygons in a dynamic coastal environment. *Ecosphere*, *2*(6), art71. https://doi.org/10.1890/ES10-00186.1

Young, D. R., Erickson, D. L., & Semones, S. W. (1994). Salinity and the small-scale distribution of three barrier island shrubs. *Canadian Journal of Botany*, *72*(9), 1365–1372. https://doi.org/10.1139/b94-167

Youngf, D. R., Shao, G., & Brinson, M. M. (1995). The Impact of the October 1991 Northeaster Storm on Barrier Island Shrub Thickets (Myrica cerifera). *Journal of Coastal Research*, *11*(4), 1322–1328.

Zinnert, J. C. (2022). *Land cover for the barrier islands of the Delmarva Peninsula in Virginia, 1984-2016* [dataset]. Environmental Data Initiative. https://doi.org/10.6073/PASTA/33E7D2BE0831FB4C09C45D780E16E596

Zinnert, J. C., Nippert, J. B., Rudgers, J. A., Pennings, S. C., González, G., Alber, M., Baer, S. G., Blair, J. M., Burd, A., & Collins, S. L. (2021). State changes: Insights from the US Long Term Ecological Research Network. *Ecosphere*, *12*(5), e03433.

Zinnert, J. C., Shiflett, S. A., Via, S., Bissett, S., Dows, B., Manley, P., & Young, D. R. (2016). Spatial–temporal dynamics in barrier island upland vegetation: The overlooked coastal landscape. *Ecosystems*, *19*(4), 685–697. https://doi.org/10.1007/s10021-016-9961-6

Zinnert, J. C., Shiflett, S. A., Vick, J. K., & Young, D. R. (2011). Woody vegetative cover dynamics in response to recent climate change on an Atlantic coast barrier island: A remote sensing approach. *Geocarto International*, *26*(8), 595–612. https://doi.org/10.1080/10106049.2011.621031

Zinnert, J. C., Via, S. M., Nettleton, B. P., Tuley, P. A., Moore, L. J., & Stallins, J. A. (2019). Connectivity in coastal systems: Barrier island vegetation influences upland migration in a changing climate. *Global Change Biology*, *25*(7), 2419–2430. https://doi.org/10.1111/gcb.14635